W.G. Jiang, C.A. Xiong, X.G. Wu

SIZE DEPENDENCE OF RESIDUAL THERMAL STRESSES IN MICRO MULTILAYER CERAMIC CAPACITORS BY USING FINITE ELEMENT UNIT CELL MODEL INCLUDING STRAIN GRADIENT EFFECT

School of Aeronautical Manufacturing Engineering, Nanchang Hangkong University, Nanchang 330063, People's Republic of China; E-mail: jiangwugui@gmail.com

Abstract. The residual thermal stresses induced by the high-temperature sintering process in multilayer ceramic capacitors (MLCCs) are investigated by using a finite element unit cell model, in which the strain gradient effect is considered. The numerical results show that the residual thermal stresses depend on the lateral margin length, the thickness ratio of the dielectrics layer to the electrode layer, and the MLCC size. At a given thickness ratio, as the MLCC size is scaled down, the peak shear stress reduces significantly and the normal stresses along the length and thickness directions change slightly with the decrease in the ceramic layer thickness t_d as $t_d > 1$ μm, but as $t_d < 1$ μm, the normal stress components increase sharply with the increase in t_d. Thus, the residual thermal stresses induced by the sintering process exhibit strong size effects and, therefore, the strain gradient effect should be taken into account in the design and evaluation of MLCC devices.

Key words: multilayer ceramic capacitor, residual stress, strain gradient plasticity, size effect, unit cell model, finite element method.

1. Introduction.

As an important type of surface-mount devices, the multilayer ceramic capacitors (MLCCs) have been widely used in a broad range of applications from household devices to satellites because of their advantages of high capacitance density and small device size [1, 2]. A MLCC has a so-called "brick" structure consisting of dielectric ceramic layers ($BaTiO_3$) and internal metallic electrodes (Ni), which are laminated alternately with each other and co-fired at a high temperature up to about 1200°C. The high-temperature sintering is an important step in fabrication process of MLCCs. After sintering, the component is cooled down to room temperature. Residual stress induced during the preparation processing could not be completely relaxed, which may cause damage and failure of the systems [3, 4].

Saito and Chazono [4] investigated uniaxial compressive stress and electric field responses of X5R-type MLCCs, and their results showed that the capacitance changes of the MLCCs have a considerable dependence on the stresses. As the number of dielectric layers increases up to 500 and the dielectric layer thickness decreases to several microns, however, it becomes more and more difficult to exactly characterize the detailed residual stress state in MLCCs via experiments. Alternatively, the finite element method (FEM) is always efficiently used to deal with these complicated problems [2, 5 – 8]. However, for a large number of the dielectric layers (e.g., 200 or even more) and a very small thickness of each layer (e.g., 1 μm or even thinner), a full three-dimensional (3D) FEM simulation of the sintering process of MLCCs requires a large number of discrete elements and a long computation time. Jiang et al. [6] and Shin et al. [8] had simulated the residual thermal stress using a full 3D FE model. However, these full 3D FE models can't capture the exact information at the tip of the inner electrodes because coarse mesh densities were used there. For multilayer

devices, a widely used method is to construct a unit cell model with periodic boundary conditions. Our previous theoretical [9] and numerical studies [6] have indicated that all the magnitudes of residual stresses increase with the increase in the layer numbers up to about 200 layers, then approach to constants with the further increase of the layer number. Therefore, for MLCCs which contain over 200 dielectric layers, a unit cell model is efficient for estimating the residual thermal stresses in a MLCC under thermal loads.

Nowadays, as a development trend in MLCCs, miniaturization requires a single layer in a MLCC become thinner and thinner. The metal electrode materials have been found to exhibit a large plastic deformation near the electrode tips [6]. For a very small thickness of each layer (e.g., 1 μm or even thinner), the classical finite element method does not include intrinsic material lengths, and is doubtful for predicting the mechanical behaviour of the MLCCs at the micron and sub-micron scales. The size-dependent material behaviour has been observed in these scale regions [10], which have been owed to geometrically necessary dislocations (GND) associated with non-uniform plastic deformation in small volumes [11]. Strain gradient plasticity theories have been developed based on the notion of GND. Also based on the Taylor dislocation model [12], a lower-order, conventional theory of mechanism-based strain gradient plasticity (CMSG) was developed by Huang et al. [13], which does not involve higher-order stress nor additional boundary conditions. To our knowledge, little work has been conducted on applying the CMSG to analyze the thermal-mechanical problems.

The present study is aimed at investigating the influence of size scale on the residual stresses induced by high-temperature processing, and thus figuring out what critical issues would appear during further miniaturization of MLCCs for guiding the design of the MLCCs. A two-dimensional (2D) axisymmetric unit cell FE model with periodic conditions along the thickness direction is proposed to examine the influences of the lateral margin length, the single layer thickness, as well as the capacitor size on the residual stresses in MLCCs, in which the thermal-mechanical CMSG is included.

2. FE model.

2.1 Unit cell model for MLCCs under thermal load. A 2D axisymmetric unit cell model was constructed using the commercial finite element program ABAQUS 6.9. A MLCC structure consists of the active region, the housing margins and the lateral margins, as shown in Fig 1, *a*.

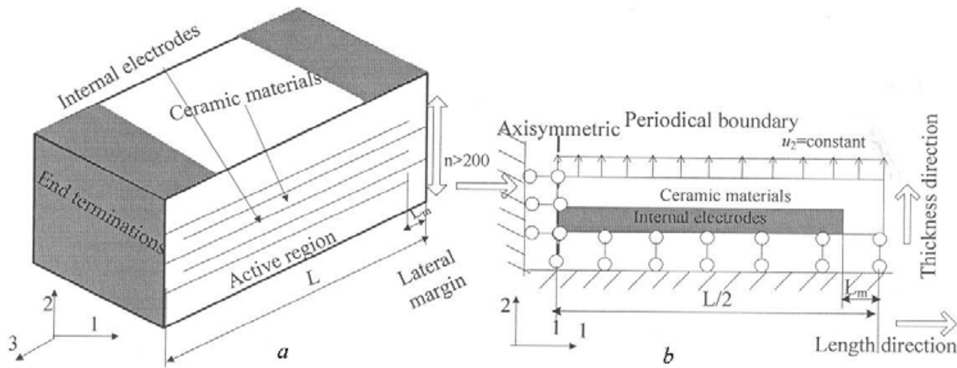

Fig. 1. Schematic structure of a MLCC and (b) its unit cell model.

The geometry of a MLCC is symmetric with respect to the *2*- and *3*-axes but asymmetric with respect to the *1*-axis because the left and the right margins have alternating electrodes (Fig 1, *a*). Franken *et al.* [5] and Prume *et al.* [7] presented a 2D plane-stress finite

element (FE) model to simulate the behavior of MLCCs and predict their reliability during soldering and bending. Shin *et al.* [8] calculated the residual stresses in the active region of a MLCC based on 2D plane-strain assumption. However, from our previous full 3D FE numerical results [6] it can be shown that axisymmetric assumption is more reasonable than plane stress or plane strain assumption. Therefore, for simplicity, it is assumed that a MLCC is axisymmetric with respect to the thickness direction (i.e. *2*-axis) of the MLCCs in our simulations. A unit cell axisymmetric model with periodical boundary is built, as shown in Fig. 1, *b*.

The initial temperature is set to 1250°C, a typical sintering temperature for $BaTiO_3$ based MLCCs, and the final temperature is set to room temperature, 20°C. Axisymmetrical 8-node bilinear element using reduced integration (CAX8R) was adopted for capturing more accurate stress fields. The deformation behavior of the dielectric ceramic layers was assumed to be elastic, while the Ni electrode was considered to be an elastic-plastic material including strain gradient effect.

2.2 Thermal-mechanical coupled constitutive law including strain gradient effect. The shear flow stress τ is related to the dislocation density ρ by [12]

$$\tau = \alpha\mu b\sqrt{\rho}\,, \tag{1}$$

where μ is the shear modulus, b is the magnitude of Burgers vector, and α is an empirical coefficient around 0,3. The dislocation density ρ is composed of the density ρ_s for statistically stored dislocations (SSDs), and the density ρ_G for geometrically necessary dislocations (GND) [14],

$$\rho = \rho_s + \rho_G\,, \tag{2}$$

ρ_G is defined as [12]

$$\rho_G = \bar{r}\frac{\eta^{\mathrm{p}}}{b}\,, \tag{3}$$

where $\bar{r}$ is the Nye-factor to reflect the scalar measure of geometrically necessary dislocations density, and $\bar{r}$ is around 1.90 for face-centered-cubic (FCC) polycrystals. η^{p} is effective plastic strain gradient, given by [13]

$$\eta^{\mathrm{p}} = \int \dot{\eta}^{\mathrm{p}} dt\,; \quad \dot{\eta}^{\mathrm{p}} = \sqrt{\frac{1}{4}\dot{\eta}^{\mathrm{p}}_{ijk}\dot{\eta}^{\mathrm{p}}_{ijk}}\,; \quad \dot{\eta}^{\mathrm{p}}_{ijk} = \dot{\varepsilon}^{\mathrm{p}}_{ik,j} + \dot{\varepsilon}^{\mathrm{p}}_{jk,i} - \dot{\varepsilon}^{\mathrm{p}}_{ij,k}\,, \tag{4}$$

where $\dot{\varepsilon}^{\mathrm{p}}_{ij}$ is plastic strain rate tensor.

The flow stress σ_{flow} accounting for the nonuniform plastic deformation associated with geometrically necessary dislocations, is defined as

$$\sigma_{\mathrm{flow}} = \sqrt{\left[\sigma_{\mathrm{ref}} f\left(\varepsilon^{\mathrm{p}}, T\right)\right]^2 + M^2\bar{r}\alpha^2\mu^2 b\eta^{\mathrm{p}}} = \sigma_{\mathrm{ref}}\sqrt{f^2\left(\varepsilon^{\mathrm{p}}, T\right) + l\eta^{\mathrm{p}}}\,, \tag{5}$$

where

$$l = M^2\bar{r}\alpha^2\left(\frac{\mu}{\sigma_{\mathrm{ref}}}\right)^2 b \tag{6}$$

is the intrinsic material length in strain gradient plasticity, M = 3,06 and $\bar{r}$ =1,90 σ_{ref} is a reference stress in plasticity (e.g., yield stress). f is a non-dimensional function of plastic

strain ε^P and temperature T. In this study, we assumed that the material parameters are time-independent, so the stress-strain relation in uniaxial tension takes the form as,

$$\sigma_{\text{flow}} == \sigma_Y \left(1+\frac{E\varepsilon^P}{\sigma_Y}\right)^N , \tag{7}$$

where E is the Young's modulus, σ_Y is the initial yield stress, and N is the plastic work hardening exponent. In order to determine ρ_s, we examine uniaxial tension, which has a vanishing plastic strain gradient $\eta_P = 0$. ρ_s is determined as

$$\rho_S = \left[\frac{\sigma_{\text{ref}} f\left(\varepsilon^P\right)}{M\alpha\mu b}\right]^2 . \tag{8}$$

For an elastic-plastic material under thermal load, the strain rate $\dot{\varepsilon}_{ij}$ is decomposed into the elastic, plastic and thermal parts.

$$\dot{\varepsilon}_{ij} = \dot{\varepsilon}_{ij}^e + \dot{\varepsilon}_{ij}^p + \dot{\varepsilon}_{ij}^{th} . \tag{9}$$

The elastic strain rate $\dot{\varepsilon}_{ij}^e$ is obtained from the stress rate $\dot{\sigma}_{ij}$,

$$\dot{\varepsilon}_{ij}^e = \frac{1}{2\mu}\dot{\sigma}_{ij}^{'} + \frac{\dot{\sigma}_{kk}}{9K}\delta_{ij} , \tag{10}$$

where $\dot{\sigma}_{ij}^{'}$ is deviatoric stress rate and K is bulk moduli. The plastic strain rate $\dot{\varepsilon}_{ij}^P$ is proportional to the deviatoric stress $\sigma_{ij}^{'}$ in the conventional J_2-flow theory of plasticity,

$$\dot{\varepsilon}_{ij}^{\text{P}} = \frac{3\dot{\varepsilon}^P}{2\sigma_e}\sigma_{ij}^{"} , \tag{11}$$

where $\sigma_e = \sqrt{3\sigma_{ij}^{"}\sigma_{ij}^{"}/2}$ is the von Mises effective stress, and $\dot{\varepsilon}^P = \sqrt{2\dot{\varepsilon}_{ij}^P\dot{\varepsilon}_{ij}^P/3}$ is the equivalent plastic strain rate.

Thermal strain rate $\dot{\varepsilon}^{th}$ due to thermal mismatch is determined by

$$\dot{\varepsilon}^{th} = \beta\dot{T} , \tag{12}$$

where $\dot{T}$ is the temperature change rate and β is the coefficient of thermal expansion (CTE).

The above CMSG considering thermal-mechanical coupling is embedded into ABAQUS by using the user subroutines UMAT and UEXPAN. The material properties used in the present simulations are listed in Table 1.

Table 1. Material parameters used in the present simulations

Materials	$BaTiO_3$	Nickel
Young's modulus E (GPa)	108	210
Poisson's ratio ν	0,25	0,33
CTE β (10^{-6}/deg)	8	13,5
Yield strength σ_Y (MPa)		690
Work hardening coefficient *N*		0,15
Burger vector *b* (Å)		2,4918
Intrinsic material length *l* (μm)		5,27

3. Results and Discussion.

3.1 Effect of the lateral margin length. A typical contour plot of the stress components is shown in Fig. 2. For the MLCC, the distributions of the various stress components including the strain gradient plasticity are shown in Fig. 2, which illustrates that ceramic materials have a large deformation around the electrode. Because the singularity is unavoidable in the interface corner between the electrode and the ceramics, the same mesh density is used in all the simulations to possibly reduce the error due to the singularity during comparison. From Fig. 2, *a*, it can be seen that the radial stress σ_{11} in most of the electrode layers is tensile. Similarly, the normal stress σ_{11} along the length direction in the ceramic layer is mostly compressive. Fig. 2, *b,* indicate that the normal stress σ_{22} along the thickness direction and shear stress σ_{12} in most of the $BaTiO_3$/Ni interface are continuous, but they change to be discontinuous severely near the electrode tips. In other words, the interface between the ceramic layer and the electrode layers near the internal electrode tips is more likely to be torn.

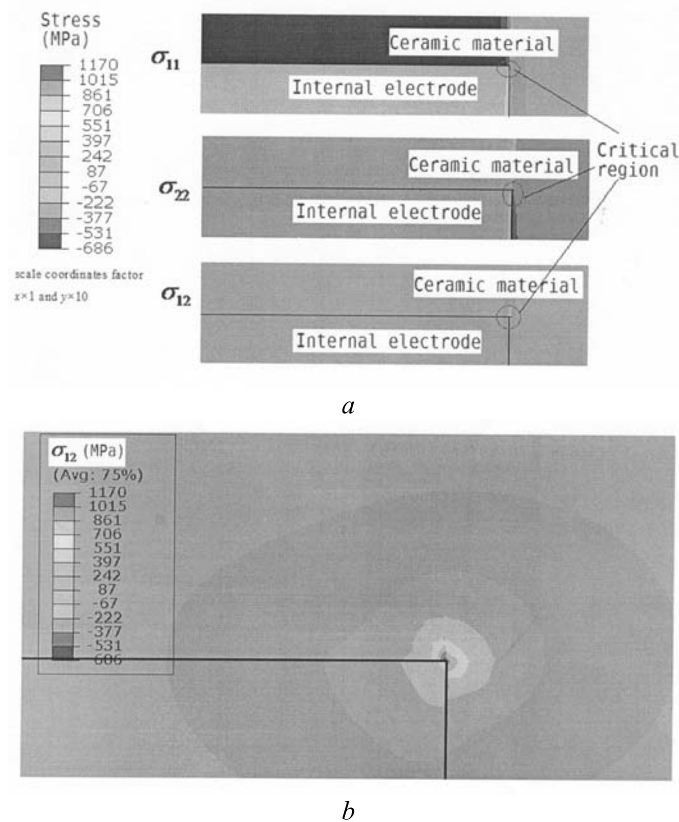

Fig. 2. (a) Contour plot of the stress components and (b) the shear stress contour near the electrode tip for the case that t_d=2 μm and t_e=2 μm (scale coordinates factor x×1 and y×10).

Better understanding the effects of the lateral margin length on the residual stresses is important for the design of MLCC structures [15], which has been investigated theoretically by Jiang *et al.* [9]. In this section, we focus on the peak stresses near the internal electrode tip using our proposed model. The length of the lateral margin L_m is varied from 10, 20, 30, 40 to 50 μm, where the dielectric layer thickness t_d is 1 μm, the electrode layer t_e is 1 μm, and L=300 μm. It is found that with the increase in the lateral margin length L_m, all of the stress components increase, because of the enhancing constraint near the electrode tip, as shown in Fig. 3.

The capacitance of an MLCC is proportional to the area of its active region. The above results show that a higher capacitance can be achieve by decreasing the lateral margin length L_m, but bigger peak residual stresses near the internal electrode tips will also be caused synchronously. Therefore, the optimal sizes of the lateral margin in MLCCs should be determined by considering the balance of the capacitance and residual stresses.

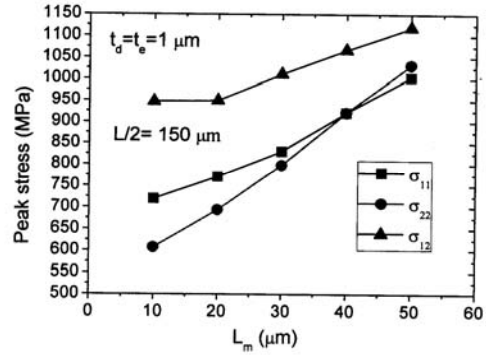

Fig. 3. Variations of the peak residual stresses near the electrode tip with respect to the lateral margin length.

3.2 Effect of the thickness ratio of the dielectrics layer to the electrode layer. For a representative electrode layer thickness (t_e=1 μm), the change of the residual stresses in MLCCs with respect to the thickness of each dielectric ceramic layer in the range of 0,3 – 3,0 μm were calculated, as shown in Fig. 4, where L = 150 μm and L_m=30 μm. From Fig. 4, *a*, it is seen that for a specified thickness of the electrode layers, in the majority of the ceramic layer of the active region, the magnitudes of the residual normal stress components along both length and thickness directions increase significantly with the decrease in the dielectric layer thickness, while the shear stress is almost zero and thickness-independent. Fig 4, *b* shows that near the electrode tip, the peak normal stresses along the length and thickness directions decrease gradually, but oppositely, the shear stress increases sharply.

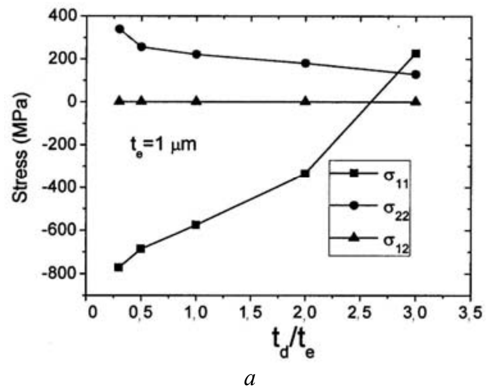

a

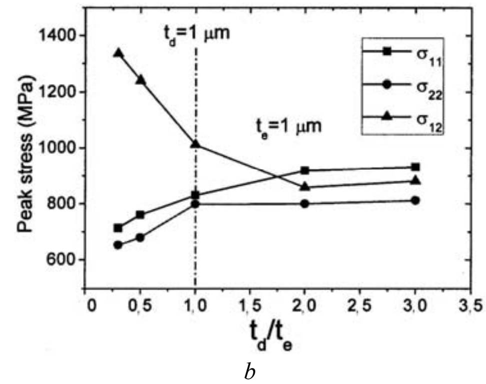

b

Fig. 4. (a) Variations of the residual stresses in the active region of the dielectric ceramic layer and (b) variations of the peak stresses near the electrode tip as a function of the thickness ratio in case of t_e=1 μm.

Considering these factors comprehensively, we can draw a conclusion that for a specified thickness of electrode layers, decreasing the ceramic layer thickness (i.e., decreasing the thickness ratio of the ceramic layer to the electrode layer) may cause the increase in the residual thermal stresses in the MLCC during the sintering process, which is against the further miniaturization of the MLCCs.

3.3 Effect of size-scale. Our previous [6] and present results suggest that the residual stress concentration is closely related to the relative thickness of the dielectric ceramic layer with respect to the electrode layer, and therefore a possible approach to decrease the ceramic layer thickness t_d without the failure of MLCC devices is to decrease the electrode layer thickness t_e simultaneously. If the thickness ratio of the ceramic layer to the electrode layer is kept to be a constant (i.e., the thicknesses of the electrode layer and ceramic layer decrease simultaneously), the change trend of the residual thermal stresses induced by the sintering process with the decrease in the single layer thickness, is not clear until now.

Table 2. Geometric parameters for investigating the size effect

	Case 1	Case 2	Case 3	Case 4	Case 5	Case 6
t_d (μm)/t_e (μm)	10/10	5/5	2/2	1/1	0.5/0.5	0.1/0.1
L/2 (μm)	1500	750	300	150	75	15
L_m (μm)	300	150	60	30	15	3

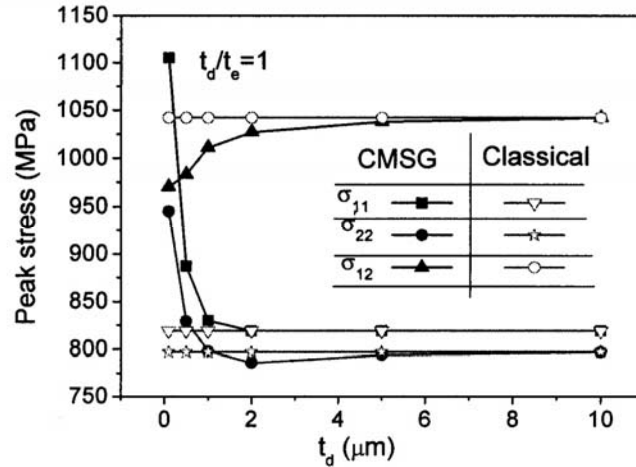

Fig. 5. Comparison of the residual thermal stresses obtained between by the present model and by the classical FE results with respect to the single layer thickness, where the MLCC size is scaled down.

In this section, the thicknesses of the ceramic and electrode layers reduce to micron and submicron scale, where the MLCC size is scaled down accordingly, as depicted in Table 2. The same thickness ratio of the dielectrics layer to the electrode layer, 1,0, is kept in all cases in our simulations. From Fig. 5, it can be seen that near the internal electrode tip, if without CMSG being considered, the peak residual thermal stresses are size independent, while if with CMSG being considered, the peak stresses are almost size- independent above 2 μm and exhibit a strong size effect below 1μm. Fig. 5 clearly demonstrates that for a given thickness ratio, as the MLCC size is scaled down, the peak shear stress reduces significantly and the normal stresses along the length and thickness directions change slightly with the decrease in the single layer thickness t_d as t_d >1 μm, but as t_d <1 μm, the normal stress components increase sharply with the further decrease in t_d. In other words, the reduction of the single layer thickness is benefit to the relaxation of the residual stress when the single layer thickness t_d is above 1 μm, but when t_d is below 1 μm, the excessive rapid increase in the residual thermal normal stresses along the length and thickness directions could cause the cracking of the brittle dielectric ceramic layers near the electrode tip. The numerical results based on the conventional FEM can not present this size effect on residual thermal stresses induced by the sintering process in micro MLCCs.

4. Conclusions.

The residual thermal stresses induced by the high-temperature sintering process in multilayer ceramic capacitors (MLCCs) were investigated by using a finite element unit cell model, in which the CMSG thermal-mechanical coupling is considered. The unit cell model with periodic boundary conditions along the thickness direction was proposed to represent the multilayer structure effect. The effects of the lateral margin length, the thickness ratio of the dielectrics layer to the electrode layer, as well as the size-scale dependence on the residual thermal stresses were all examined. Some conclusions can be drawn as follow:

1. The normal stress along the thickness direction and the shear stress in most of the ceramics/electrode interface are continuous, but they change to be discontinuous severely near

the electrode tips. In other words, the interface between the ceramic layer and the electrode layers is more likely to be torn near the internal electrode tips.

2. A higher capacitance can be achieve by decreasing the lateral margin length L_m, but bigger peak residual stresses near the internal electrode tips will also be caused synchronously. Therefore, the optimal sizes of the lateral margin in MLCCs should be determined by considering the balance of the capacitance and residual stresses.

3. For a specified thickness of electrode layers, decreasing the ceramic layer thickness (i.e., decreasing the thickness ratio of the ceramic layer to the electrode layer) may cause the increase in the residual thermal stresses in the MLCC during the sintering process, which is against the further miniaturization.

4. For a given thickness ratio, as the MLCC size is scaled down, the peak shear stress reduces significantly and the normal stresses along the length and thickness directions change slightly with the decrease in the single layer thickness t_d as t_d >1 μm, but as t_d <1 μm, the normal stress components increase sharply with the continued decrease in t_d. In other words, the reduction of the single layer thickness is benefit to the relaxation of the residual stress when the single layer thickness t_d is above 1 μm, but when t_d is below 1 μm, the excessive rapid increase in the residual thermal normal stresses along the length and thickness directions could cause the cracking of the brittle dielectric layers near the electrode tip.

5. The residual thermal stresses induced by the sintering process exhibit strong size effects and, therefore, strain gradient effect should be taken into account in the design and evaluation of MLCC devices.

ACKNOWLEDGMENTS.

This work was supported by the National Science Foundation of China (10902048), the Foundation of Jiangxi Educational Committee (GJJ08229) and the Natural Science Foundation of Jiangxi Province (2008GZW0010). The first author would appreciate the excellent advice from Dr. S. Qu.

Р Е З Ю М Е . Розглянуто задачу про залишкові температурні напруження в багатошарових керамічних конденсаторах, викликані високотемпературним процесом спікання. Застосовано модель одиничної чарунки в методі скінченних елементів, де враховано вплив градієнта деформацій. Отримані числові результати показують, що залишкові температурні напруження залежать від довжини поздовжнього краю, відношення товщини діелектричних шарів до товщини електродних шарів і розміру конденсатора. При заданому відношенні товщин, коли розмір конденсатора зменшується, то найвищі зсувні напруження зменшуються суттєво і нормальні напруження вздовж довжини та в напрямку зміни товщини змінюються незначно зі зменшенням товщини керамічного шару до величини, меншої 1 мікрона. Коли ця величина є більшою 1 мікрона, то нормальні напруження зростають різко зі збільшенням товщини керамічного шару. Таким чином, залишкові температурні напруження, викликані високотемпературним процесом спікання, виявляють сильний вплив розміру конденсатора і тому вплив градієнта деформації повинен братися до уваги в процесі створення і оцінювання роботи багатошарових керамічних конденсаторів.

1. *Chen X.C., Huang X.Y.* The research situation and development prospect of MLCC // Materials Review. – 2004. – **18**. – P. 12 – 14.
2. *Jiang W.G., Feng X.Q., Nan C.W.* Influence of residual thermal stresses and geometric parameters on stress and electric fields in multilayer ceramic capacitors under electric bias // J. of Phys. D Appl. Physics. – 2008. – **41**. – P. 135 – 310.
3. *Hao T.H., Gong X., Suo Z.* Fracture mechanics for the design of ceramic multilayer actuators // J. of Mech. and Phys. of Sol. – 1996. – **44**. – P. 23 – 48.
4. *Saito K., Chazono H.* Stress and electric field responses of X5R type multilayer ceramic capacitor with Ni internal electrode // Japanese J. of Appl. Physics. – 2003. – **42**. – P. 6045 – 6049.
5. *Franken K., Maier H.R., Prume K., Waser R.* Finite-Element analysis of ceramic multilayer capacitors: failure probability caused by wave soldering and bending loads // J. of the Amer. Ceramic Soc. – 2000. – **83**. – P. 1433 – 1440.

6. *Jiang W.G., Feng X.Q., Yang G., Yue Z.X., Nan C.W.* Influences of thickness and number of dielectric layers on residual stresses in micro multilayer ceramic capacitors // J. of Appl. Physics. – 2007. – **101**(10). – P. 104 – 117.
7. *Prume K., Franken K., Bottger U., Waser R., Maier H.R.* Modelling and numerical simulation of the electrical, mechanical, and thermal coupled behaviour of multilayer capacitors (MLCs). – J. of the European Ceramic Society. – 2002. – **22**. – P. 1285–1296.
8. *Shin H., Jung J.S., Hong K.S.* Investigation of useful or deleterious residual thermal stress component to the capacitance of a multilayer ceramic capacitor // Microelectronic Engineering. – 2005. – **77**. – P. 270 – 276.
9. *Jiang W.G., Feng X.Q., Nan C.W.* A three-dimensional theoretical approach for estimating the thermal residual stress in multilayer ceramic capacitors // Composites Science and Technology. – 2008. – **68**. – P. 692 – 698.
10. *Gouldstone A., Chollacoop N., Dao M., Li J., Minor A.M., Shen Y.L.* Indentation across size scales and disciplines: recent developments in experimentation and modelling // J. Acta Materialia. – 2007. – **55**. – P. 4015 – 4039.
11. *Nix W.D., Gao H.* Indentation size effects in crystalline materials: A law for strain gradient plasticity // J. of the Mechanics and Physics of Solids – 1998. –**46**. – P. 411 – 425.
12. *Taylor G.I.* The mechanism of plastic deformation of crystals Part I.-theoretical // J.
Proceedings of the Royal Society of London A. – 1934. – **145**. – P. 362 – 387.
13. *Huang Y., Qu S., Hwang K. C., Li M., Gao H.* A conventional theory of mechanism-based strain gradient plasticity // Int. J. of Plasticity. – 2004. – **20** – P. 753 – 782.
14. *Qu S., Huang Y., Pharr G.M., Hwang K.C.* The indentation size effect in the spherical indentation of iridium: a study via the conventional theory of mechanism-based strain gradient plasticity // Int. J. of Plasticity. – 2006. – **22**. – P. 1265 – 1286.
15. *Shin H., Park J.S., Hong K.S., Jung H.S., Lee J.K., Rhee K.Y.* Physical origin of residual thermal stresses in a multilayer ceramic capacitor // J. Appl. Physics. – 2007. – **101.** – P. 063 – 527

From the Editorial Board: The article corresponds completely to submitted manuscript.

Поступила 06.09.2010 Утверждена в печать 26.06.2013